J Bionic Eng 15 (2018) 83–93
DOI: https://doi.org/10.1007/s42235-017-0006-4

Functional Design for Customizing Sit-To-Stand Assisting Devices

Pierluigi Rea, Erika Ottaviano*

DICeM-Department of Civil and Mechanical Engineering, University of Cassino and Southern Lazio, via Di Biasio 43, 03043 *Cassino* (*FR*), *Italy*

Abstract

Standing up refers to the transition from the seating to the standing postures to perform a movement that involves several body segments and requires both voluntary action and equilibrium control during an important displacement of the body Centre of Gravity (COG). This task can be considered very important for people with reduced mobility to achieve minimal independence in Activity of Daily Living (ADL). In this paper, we propose solutions for the homecare of persons with reduced mobility, describing a functional design to customize assisting devices for the Sit-to-Stand (STS). In particular, the support mechanism that generates the requested motion and sustains the body of a person can be synthesized ad-hoc according to the experimental data of the subject. Experimental tests carried out during the Sit-To-Stand are used to track and record point trajectories and the orientation of the trunk of an individual, and they are used to design a 1-DOF mechanism able to reproduce the assigned rigid-body motion. A four-bar linkage has been synthesized according to the desired features. Simulation results are reported to illustrate the engineering soundness of the proposed mechatronic solution.

Keywords: assisting device, Sit-to-Stand, bionic design, kinematic synthesis, experimental evaluation, simulation

1 Introduction

According to the UN's World Population Prospects the proportion of Europeans aged 65 years and older will grow from 16% in 2000 to 24% by 2030[1]. Life Expectancy (LE) is also increasing, particularly in the richer European countries[2]. The rapid growth of aging populations and LE have put a great pressure on the healthcare infrastructure, and providing comprehensive care to an aging population can be considered as global concern. One key point to improve the quality of life of individuals is to help them in keeping some form of independence in ADL, which consists of self-care tasks including hygiene, dressing, toileting, transferring, and self-feeding. STS is part of transferring, and despite its apparent simplicity, it is a mechanically demanding functional task undertaken daily, requiring a strong coordination between posture and movement. Unfortunately, due to several reasons, it may represent a problem for people with a reduced mobility. Assistive devices are developed to enhance basic motor activities, such as postural changes or walking.

In this paper, we focus our interest in the development of new solutions for STS devices for the homecare of the elderly and people with reduced mobility with the further advantage of relieve the work of caregivers. The end-users of the addressed robotic system are persons with reduced mobility due to physiological degradation of the motor system by aging or because of neurological diseases who need assistance at home.

Rehabilitating and assistive technologies are evolving rapidly thanks to scientific and technological innovation and the availability of systems. Assistive systems for aiding basic motor activities such as postural change are lifting cranes or lifting belts. Assistive devices have been developed for more complex tasks, such as walking and feeding. In the related literature, the analysis of kinetic data of the body movement and skeletal motion during the STS has been subject of several studies[3–5]. Redesign of the STS assistive devices to mimic normal or natural-like STS transfer can promote safety for the patient and the caregiver[6]. Devices have been conceived to assist people during the walk operation[7], aiding during the STS[8–11], for human–robot interaction[12]. Available motion aiding systems are re-

***Corresponding author:** Erika Ottaviano
E-mail: ottaviano@unicas.it

ported in Refs. [13,14].

An assisting robotic device is given in Ref. [15]. The concept of using exoskeletons is presented in Ref. [16]. Despite of very positive results, some of the developed solutions have high complexity/cost/encumbrance. Moreover, the concept of customization can be considered of interest in the assistive technology market and STS devices, for which it can be interesting to have a system easy to adjust to the height of the subject. More specifically, the only solution available on the market for the above-mentioned concept refers to handle bars that can be adjusted to the height of the person[17]. A solution in Ref. [18] reproduces a STS motion pattern with constant orientation. In this paper, we address a novel concept of designing the supporting mechanism in order to customize a device for an individual. We propose a methodology according to the needs of an individual, but limiting the number of the Degrees of Freedom (DOF) of the support mechanism that generates the motion. The design procedure can be summarized as follows: (1) acquisition of experimental data of the STS; (2) type and dimensional synthesis of the support mechanism; (3) mechanical design; (4) simulation for verification. Experimental tests of the STS were obtained by using a 3D motion capture system based on cameras. A suitable planar mechanism is synthesized. Among several solutions, we choose to simplify the support mechanism to reduce the DOFs mainly to reduce the overall cost and complexity of the control. The mechanism has been synthesized using a prescribed set of finitely separated poses taken from experimental data to solve the Burmester problem for the case understudy.

2 Experimental evaluation of the STS

A trial for the STS was carried out at the University of Cassino and Southern Lazio involving 20 healthy volunteers (age between 20 and 30, height from 1.55 m to 1.95 m). The criterion for selection of the individuals for the trial was based on the availability of voluntary subjects. In the experimental tests the individuals were asked to seat on an armless chair set to the 100% of the knee height. The back support of the chair was used to set the trunk in the vertical position. The arms did not actively participate to the STS. The subjects were asked to assume a seated position and then they were asked to stand up from the chair. The required first task is the 3D motion tracking performed without interference with the movement of an individual. Marker Based System (MBS) technology satisfies those requirements. A type of MBS is an optical motion capture system composed of infrared cameras that can track human movements thanks to a kit of reflective markers usually attached to a special MoCap suit. The advantage of using this solution is the possibility of fast and accurate tracking of a complex 3D motion. Drawbacks are mainly related to the relatively high complexity and cost, and the need of using reflecting markers that must be accurately positioned. Another solution is the use of Markerless Motion Capture (MMC) system, which shows the following advantages, there is no need to position markers, therefore no error due to makers' placements. Generally, these systems are more affordable and portable than MBS. A possible drawback of MMC deals with the accuracy of the system, which can lead to reluctance from potential clinical users. Moreover, the precision depends on the number of cameras used. In this paper, we have chosen to use the Microsoft Kinect sensor because of its advantages in terms of low-cost and easy in use. In addition, in Ref. [19] a comparison between the Microsoft Kinect with a standard motion capture technology is reported showing very good features of the Kinect providing skeletal tracking that is more robust to occlusions and body rotation. Recently, due to the high demand, there is the need for developing easy-to-use and economic systems for rehabilitation and assistive tasks, as those presented in Refs. [20,21] as well as the need to develop fast and easy-to-use systems for monitoring and determining biomechanical performances of the human body. One remarkable example for 3D motion capture is the Virtual Sensei software, which was developed as a tool for sports and biomechanical analysis of 3D fast motions[22,23]. We used the Virtual Sensei together with the Microsoft Kinect for the evaluation of the STS. The motion sequence obtained during the trial is given in Fig. 1. The movement pattern of the neck and trunk can be divided into two phases, the flexion phase (forward movement), and the extension phase (lifting movement)[4], as it can be observed from the experimental results reported in Fig. 2.

Experimental results in Fig. 2 are displayed in the video capture system reference frame with the origin located in the center of the sensor, as outcome of the Virtual Sensei. Data can be conveniently expressed in a frame attached to the subject's foot after a change of the reference frame, as it will be shown in the plots of Figs. 3 and 4. In the following, we focus the attention on the shoulder (as it is shown by marker labeled as 4) in Fig. 1) to focus the attention on that trajectory.

Experimental results show a large variation in the size trajectory, but it is always possible to recognize a typical shape, named as reference trajectory, which can be schematized by four parameters: LF, length of the forward movement, HF, height of forward movement, HL height of the lifting movement, and LL length of the lifting movement. The parameters have been measured for all the subjects. Fig. 3 shows the 14 tests performed by the male subject in Fig. 1, and Fig. 3b shows

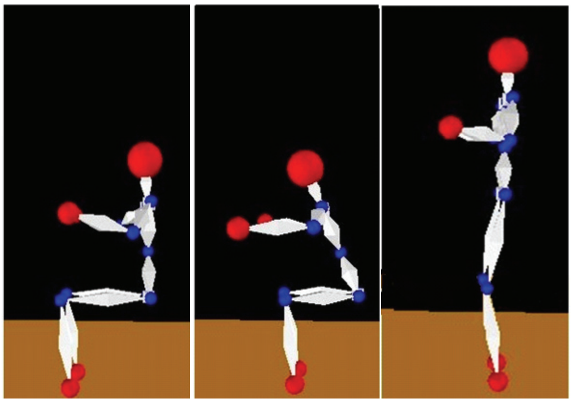

Fig. 1 A motion sequence of STS obtained by experimental trial.

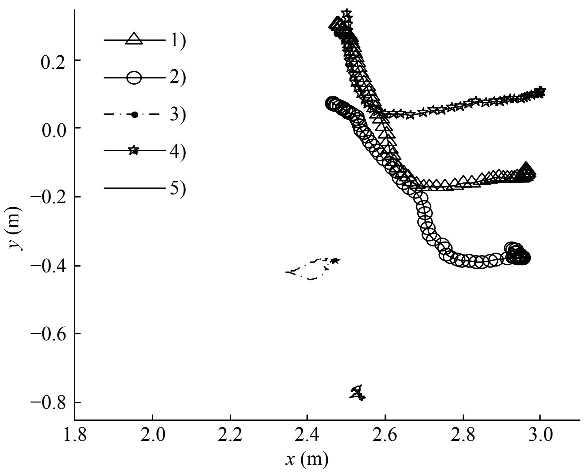

Fig. 2 Experimental test on a male subject during the STS in Fig. 1: trajectories of points of interest. (1) Chest; (2) hip; (3) knee; (4) shoulder; (5) ankle.

"reference trajectories" for male and female subjects. A reference trajectory is a simplified trajectory having the typical shape and dimensions according to the size of the subject. For the synthesis procedure, either a real or a reference trajectory can be used. In the paper, we focused our interest on a real trajectory that is selected being the closest one to the mean trajectory during the trial. The same procedure for the experimental evaluation can be used to evaluate the STS motion of persons with reduced mobility, due to age or other impairments under more specific conditions in a clinical trial. For more information about the 3D MoCap system, refer to Refs. [22,23].

3 Design requirements for STS assisting devices

The premise for the study of the STS is great variation of motion patterns, therefore, there are differences in the anthropometric data of individuals, and each has his/her own unique style of movement as distinctive of his/her personality, and also according to the age, weight strength in muscles. The myriad of factors that influence these variations are too numerous to be controlled, indeed in the context we focus the attention on a subject to design a customized transfer support mechanism integrated into the assisting device. The mechanism can be therefore designed ad-hoc facing the arising needs of person understudy. More specifically, taking into account that each person may have different trajectories each time he/she repeats the action, for the design procedure we choose a real trajectory, which is the closest to the mean trajectory, as shown in Fig. 3.

Referring to the design of a mechatronic system, it must be composed of a mechanical part for generating the requested motion with an orientation of the trunk support, an actuation system to give suitable power to lift and sustain the person, and interfaces to hold and sustain the person in a stable way. In addition, any security system has to be considered to prevent accidental falls and brake system should be included in the overall design. Mechatronic units and suitable software will complete the system.

We focus on the mechanism devoted to reproduce a desired trajectory with prescribed orientation, as the system has to accomplish the STS motion and sustain the

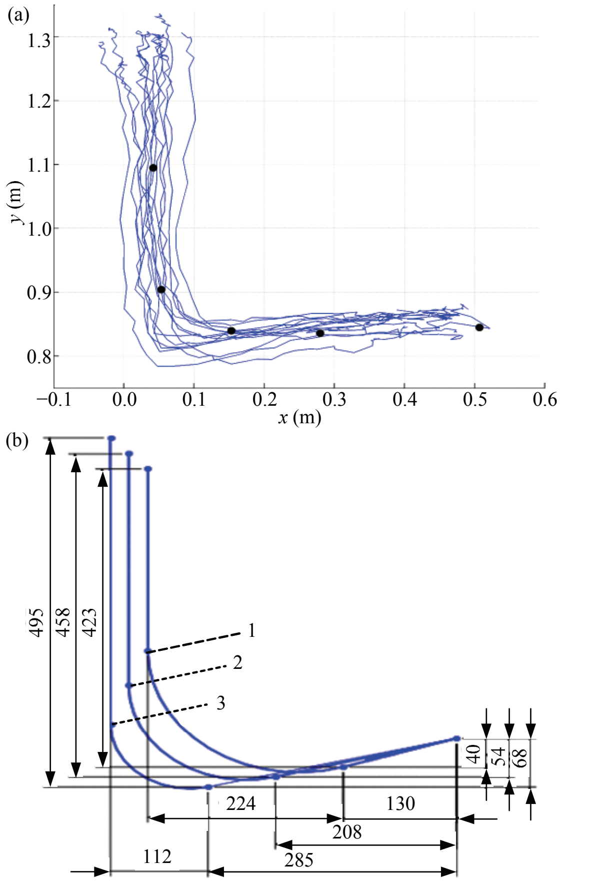

Fig. 3 Trajectories of the point at the shoulder. (a) Experimental results of the trial for a male subject (dot points are taken from the trajectory closest to the mean trajectory during the trial); (b) trajectory pattern for a male (3) and a female (1) subjects, and a reference trajectory (2), quotes are expressed in millimeters.

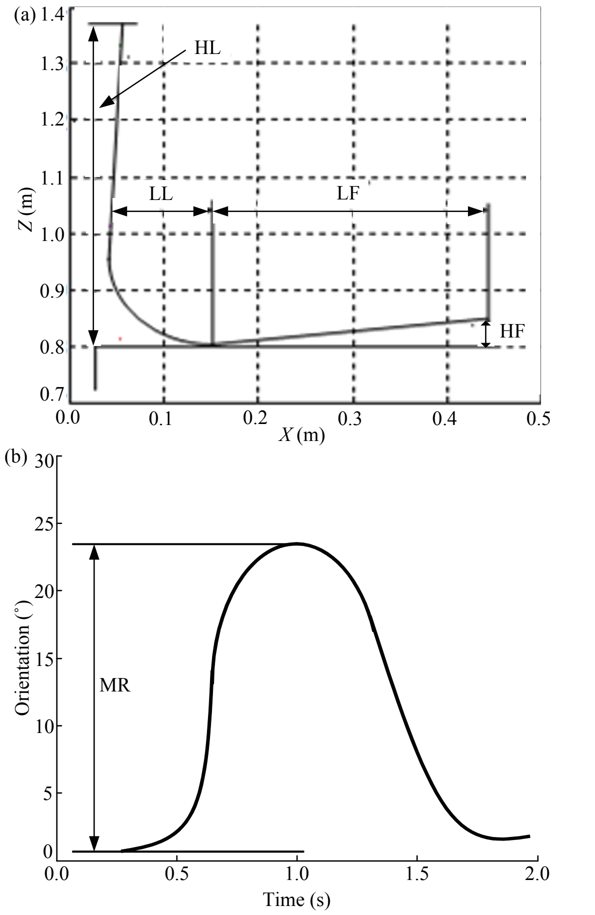

Fig. 4 A sketch and main parameters for (a) the STS trajectory pattern, (b) correspondent orientation. (HL: height of the lifting; LL: length of the lifting; LF: length of the forward; HF: height of forward; MR: max rotation of the trunk).

body of the person. The designer should find a mechanism (or linkage) that will meet the requirements that can be summarized as follows: the device should possess generally 2-DOFs in sagittal plane to accomplish any kind of requested trajectory, which vary according to anthropometric data of the subject, and his/her physical conditions. In addition, the orientation of the trunk during the movement depends by the seat and its height and physiological factors of the patient. Therefore, an additional DOF can be included to provide a suitable orientation for the trunk support. According to these requirements, a designer should identify to pology of the kinematic chain underlying the mechanical structure choosing among serial, parallel or hybrid structures. If the requested motion is in the sagittal plane, a planar mechanism instead of spatial one can be considered. Among several solutions, we have chosen to simplify the problem reducing the number of DOFs, mainly to have simpler control units and less expensive actuation system rather than a 3-DOFs system, as those described in Refs. [24,25] or cable systems[26], which can be also used as active/passive systems as pose estimation devices. Furthermore, a large number of commercialized systems are lifting cranes or lifting belts with 1-DOF only. Considering the above-mentioned arguments a four-bar linkage has been selected having 1-DOF. In order to accomplish the task of providing suitable trajectory and orientation a dimensional synthesis is required. The 4-bar linkage can be synthesized solving the Burmester problem, as it will be explained. Nevertheless, a design of a mechanism based on the trajectory pattern in Fig. 4 with related values of the movement parameters in Table 1 can be also performed discarding the orientation of the trunk.

Table 1 Values for the movement parameters of the trajectory pattern

HF:	LF:	LL:	HL:	MR:
0.053 m	0.207 m	0.168 m	0.458 m	23 deg

4 The design of a STS device

According to the requirements and constraints, we have designed a mechatronic system for the STS, as shown in Fig. 5. We have chosen to consider a planar mechanism for the support mechanism to be installed frontally and having 1-DOF in order to reproduce the rigid body motion taking into account a male subject movement included in the experimental trial through the trajectory reported in Fig. 6. The subject is chosen because his trajectory and trunk orientation represent a good mean of the tests, as shown in Fig. 3. The axis of the active joint for the support mechanism is given in Fig. 5. Nevertheless, it has to be mentioned that the design procedure that follows is specifically referred to the support mechanism, is general and can be applied for a large variety of cases of study, either to design a STS device having a customized mechanism or referring to a trajectory pattern and orientation given in Fig. 4. In particular, the orientation of the trunk has been considered together with the desired trajectory, as shown in Fig. 6, which represents the input data for the synthesis procedure. It is worth noting that points in Fig. 6 are conveniently expressed in a frame attached to the subject's foot. A rigid coupler motion problem is then addressed here in order to design a mechanism capable to lift a person maintaining at the same time a comfortable posture of the trunk during the operation.

4.1 Kinematic synthesis of the mechanism

Planar mechanisms are in general used in industrial environment for automatic machinery in order to give prescribed law of motions that are given according to the task to be performed. They can be referred as function generators from the input to the output links, rigid body guidance through the study of the rigid coupler motion, and path generators by referring to the coupler curve, as extensively reported in Refs. [27–30]. In this context it is chosen to design a four-bar linkage that guides a rigid body attached to the coupler link through N prescribed poses. It is well-known from literature that a Revolute-Revolute (RR) dyad can be synthesized exactly for up to five prescribed poses[31]. The module deals with the Burmester problem, which aims at finding the geometric parameters of a four-bar linkage required for a prescribed set of finitely separated poses. The problem can be then formulated as locating the positions of the joint centres A, A_0, B, B_0, in a way that five given poses can be visited exactly.

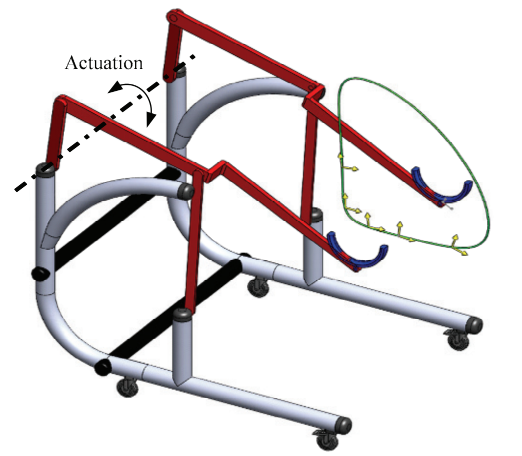

Fig. 5 A sketch for the mechanical design of the STS device.

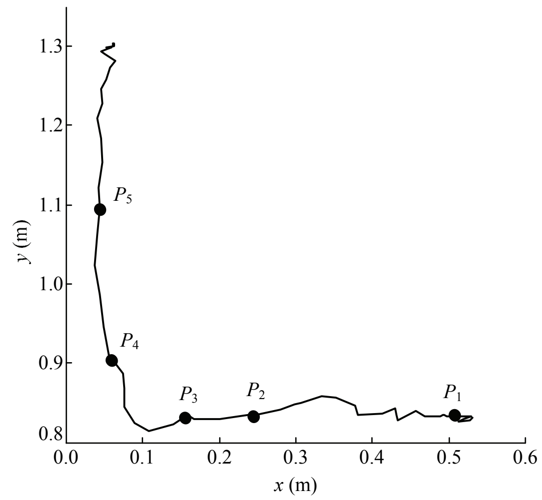

Fig. 6 Experimental result of a male subject. Dot points are the 5 chosen precision points $P_i = (x_i, y_i, \phi_t)$ for the synthesis procedure: $P_1 = (0.506, 0.843, -16)$; $P_2 = (0.279, 0.835, 0)$; $P_3 = (0.155, 0.532, 5)$; $P_4 = (0.59, 0.904, -2)$; $P_5 = (0.043, 1.094, 0)$.

The set of prescribed poses can be given with respect to a fixed frame, say OX_0Y_0 in Fig. 7, in the form ($\boldsymbol{r}_j$, θ_j), being $\boldsymbol{r}_j$ the position vector of a coupler point P at the jth pose, while θ_j defines the jth orientation of the guided body. Without loss of generality, if relative angles

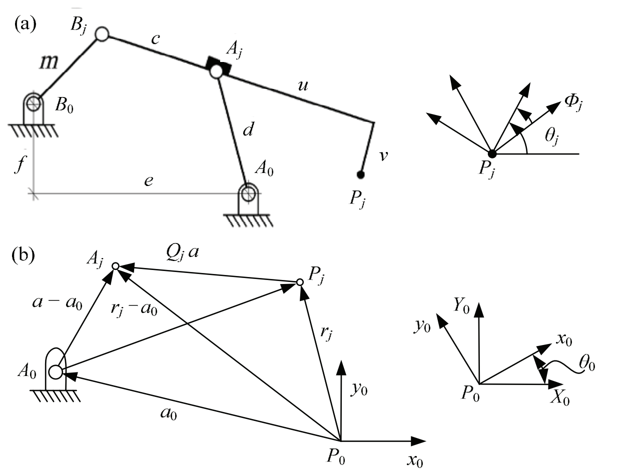

Fig. 7 A kinematic scheme for the synthesis of a four-bar linkage. (a) In the j-th pose for the rigid body guidance with respect to the (P_0, ϕ_0) reference pose; (b) relation between points and vectors of the j-th pose with those of the reference pose.

ϕ_j are expressed as $\phi_j = \theta_j - \theta_0$, and the origin O of the fixed frame is chosen as coincident with P_0 (first position of the coupler point P) as in Fig. 7b then the set of N given poses reduces to ($\boldsymbol{r}_j$, θ_j). Therefore, the remaining four poses are described with respect to a frame attached to the first one. For four poses then the problem can be formulated as a system of four algebraic equations in four unknowns, which are the x and y coordinates of the joint centres A, A_0, B, B_0. Let us consider the scheme in Fig. 7b, the condition that the distance between points A_0 and A_j remains constant can be expressed as:

$$\left\|\left(\boldsymbol{r}_j - \boldsymbol{a}_0\right) + \boldsymbol{Q}_j \boldsymbol{a}\right\| = \left\|\boldsymbol{a} - \boldsymbol{a}_0\right\|, \ j = 1, \ldots, N, \quad (1)$$

in which $\boldsymbol{a}_0$ and $\boldsymbol{a}$ represent the position vectors of points A_0 and A_j, respectively, with respect to the chosen Cartesian frame in P_0, and matrix $\boldsymbol{Q}_j$ can be expressed as:

$$\boldsymbol{Q}_j = \begin{bmatrix} \cos\phi_j & -\sin\phi_j \\ \sin\phi_j & \cos\phi_j \end{bmatrix}, \ j = 1, \ldots, N. \quad (2)$$

After squaring and expanding Eq. (1) and further algebraic manipulation the following synthesis equations can be obtained in the form:

$$f_j = \boldsymbol{a}_0^{\mathrm{T}} \left(\boldsymbol{1} - \boldsymbol{Q}_j\right) \boldsymbol{a} + \boldsymbol{r}_j^{\mathrm{T}} \boldsymbol{Q}_j \boldsymbol{a} - \boldsymbol{r}_j^{\mathrm{T}} \boldsymbol{a}_0 + \frac{\boldsymbol{r}_j^{\mathrm{T}} \boldsymbol{r}_j}{2}, \quad (3)$$

as described in Ref. [28] where $\boldsymbol{1}$ is the [2 × 2] identity matrix.

Several authors have addressed the Burmester problem, it can be solved by intersecting two curves representing the loci of the center points for two four-poses subsets out of the given five-pose set, as reported in Refs. [31,32], by applying complex numbers[33], by using kinematic mapping[34]. In the following, we have used a method based on dyalitic elimination[35], because it leads to a numerically robust algorithm that can be successfully used for many applications including the case understudy. Joint centers can be found through the intersections of the four possible contours of the four-pose problem. Thus, the system of equations in Eq. (3) can be rewritten in the form of dyalitic elimination of $\boldsymbol{a}$ being the vector of unknowns $\boldsymbol{z} = [\boldsymbol{a}^{\mathrm{T}} \ 1]^{\mathrm{T}}$.

$$\boldsymbol{M}\boldsymbol{z} = \boldsymbol{0}, \quad (4)$$

in which matrix $\boldsymbol{M}$ can be expressed as:

$$\boldsymbol{M} = \begin{bmatrix} \boldsymbol{a}_0^{\mathrm{T}}\left(\boldsymbol{1} - \boldsymbol{Q}_1^{\mathrm{T}}\right) - \boldsymbol{r}_1^{\mathrm{T}} & \boldsymbol{r}_1^{\mathrm{T}}\left(\boldsymbol{Q}_1 \boldsymbol{a}_0 + \boldsymbol{r}_1/2\right) \\ \boldsymbol{a}_0^{\mathrm{T}}\left(\boldsymbol{1} - \boldsymbol{Q}_2^{\mathrm{T}}\right) - \boldsymbol{r}_2^{\mathrm{T}} & \boldsymbol{r}_2^{\mathrm{T}}\left(\boldsymbol{Q}_2 \boldsymbol{a}_0 + \boldsymbol{r}_2/2\right) \\ \boldsymbol{a}_0^{\mathrm{T}}\left(\boldsymbol{1} - \boldsymbol{Q}_3^{\mathrm{T}}\right) - \boldsymbol{r}_3^{\mathrm{T}} & \boldsymbol{r}_3^{\mathrm{T}}\left(\boldsymbol{Q}_3 \boldsymbol{a}_0 + \boldsymbol{r}_3/2\right) \\ \boldsymbol{a}_0^{\mathrm{T}}\left(\boldsymbol{1} - \boldsymbol{Q}_4^{\mathrm{T}}\right) - \boldsymbol{r}_4^{\mathrm{T}} & \boldsymbol{r}_4^{\mathrm{T}}\left(\boldsymbol{Q}_4 \boldsymbol{a}_0 + \boldsymbol{r}_4/2\right) \end{bmatrix}. \quad (5)$$

Matrix $\boldsymbol{M}$ admits solutions different from the trivial one if $\boldsymbol{M}$ is non-singular. The determinants of the four [3 × 3] sub-matrices can be computed. Thus, the four determinants are bivariate polynomials in the two unknown components of the vector $\boldsymbol{a}_0$ and they define four curves in x-y plane. The intersection of the four curves gives all possible real solutions of the problem. In a similar procedure also the vector $\boldsymbol{a}$ can be computed. The system of equation in (3) can be rewritten being the vector of unknowns $\boldsymbol{w} = [\boldsymbol{a}_0^{\mathrm{T}} \ 1]^{\mathrm{T}}$ in a form similar to Eq. (4) in which a new matrix $\boldsymbol{N}$ can be expressed as:

$$\boldsymbol{N} = \begin{bmatrix} \boldsymbol{a}^{\mathrm{T}}\left(\boldsymbol{1} - \boldsymbol{Q}_1\right) + \boldsymbol{r}_1^{\mathrm{T}} \boldsymbol{Q}_1 & -\boldsymbol{r}_1^{\mathrm{T}}\left(\boldsymbol{a} + \boldsymbol{r}_1/2\right) \\ \boldsymbol{a}^{\mathrm{T}}\left(\boldsymbol{1} - \boldsymbol{Q}_2\right) + \boldsymbol{r}_2^{\mathrm{T}} \boldsymbol{Q}_1 & -\boldsymbol{r}_2^{\mathrm{T}}\left(\boldsymbol{a} + \boldsymbol{r}_2/2\right) \\ \boldsymbol{a}^{\mathrm{T}}\left(\boldsymbol{1} - \boldsymbol{Q}_3\right) + \boldsymbol{r}_3^{\mathrm{T}} \boldsymbol{Q}_1 & -\boldsymbol{r}_3^{\mathrm{T}}\left(\boldsymbol{a} + \boldsymbol{r}_3/2\right) \\ \boldsymbol{a}^{\mathrm{T}}\left(\boldsymbol{1} - \boldsymbol{Q}_4\right) + \boldsymbol{r}_4^{\mathrm{T}} \boldsymbol{Q}_1 & -\boldsymbol{r}_4^{\mathrm{T}}\left(\boldsymbol{a} + \boldsymbol{r}_4/2\right) \end{bmatrix}. \quad (6)$$

Once all sets of real solutions of both $\boldsymbol{a}_0$ and $\boldsymbol{a}$ have been obtained, we resort to the synthesis equations to pair of them. It can be shown that each determinant of the submatrices from Eqs. (5) and (6) is cubic, and for any of the two sets the four equations in two unknowns reduce to a quartic polynomial[31]. The solutions for $\boldsymbol{a}_0$

and $\boldsymbol{a}$ are computed independently, leading to the problem of finding the solution of overdetermined non-linear system of equations. Initial estimates are produced and then the solutions are refined numerically. According to the above-mentioned procedure, experimental results of a male subject shown in Fig. 6 are chosen as the reference rigid body motion to prescribe the set of finitely separated poses associating the orientation of trunk corresponding to each chosen precision point of Fig. 6. Then, for the five chosen poses, the numerical values of position and orientation are given in the caption of Fig. 6. It is worth to mention that coordinates of precision points P_i are given with respect to a reference system attached to a fixed point chosen on the frame support of the device. Substituting the values of the P_j coordinates and correspondent rigid body orientation described in a frame attached to P_0 (first pose) one can obtain the requested set of equations. According to the formulation, the solutions for $\boldsymbol{a}_0$ and $\boldsymbol{a}$ are computed independently but plotted together in Fig. 8, therefore, the eight curves intersect in A, A_0, B, B_0 points, which are described in a frame attached to P_0 as it is shown in Fig. 7b).

4.2 Kinematic analysis of the mechanism

It is well known in planar kinematics that the curve traced by any point of the coupler link of a planar four-bar linkage, as it is shown in Fig. 7a, is expressed by an algebraic polynomial of sixth degree[29].

Let us consider the planar mechanism in Fig. 7a in a Cartesian reference frame $A_0X_0Y_0$. The coupler link carries a point P that serves as the origin of the second Cartesian frame, with origin in P and axes X_j, Y_j fixed to this link, with a relative orientation of the frames expressed by θ. The equation of a coupler point curve for any four-bar linkage may be obtained by analytic geometry being the loci of any point P that belongs to a segment for which points A and B are constrained to lie on two circles. According to the kinematic scheme in Fig. 7a, the position of point P, with coordinates (x, y) can be described with respect to OX_0Y_0 fixed frame, as a function of kinematic parameters of the mechanism A_0AB_0BP. In particular, it can be noted that the linkage posture links A_0A (and B_0B) can be evaluated as:

$$\|A_0A\|^2 = d^2,\ \|B_0B\|^2 = m^2, \tag{7}$$

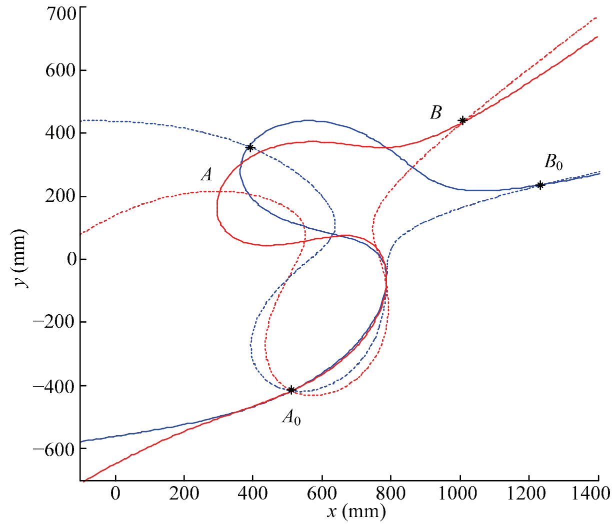

Fig. 8 The eight curves giving the x and y coordinates of A, A_0, B, B_0 points.

which can be rewritten by considering the fixed frame attached to point A_0 as:

$$\begin{cases} A_0A = \begin{bmatrix} x + u\cos\theta - v\sin\theta \\ y + u\sin\theta + v\cos\theta \end{bmatrix} \\ B_0B = \begin{bmatrix} x - e + (u+c)\cos\theta - v\sin\theta \\ y - f + (u+c)\sin\theta - v\cos\theta \end{bmatrix}, \end{cases} \tag{8}$$

and considering a rotation matrix $\boldsymbol{Q}$ in Eq. (2) that relates fixed and moving frames to express all vectors in the same reference frame. Substituting Eq. (8) in Eq. (7), one can obtain two equations, which are function of design parameters and x, y and θ in the form.

$$x^2+y^2+2[ux+vy]c\theta+2[uy-vx]s\theta+v^2+u^2-d^2=0, \tag{9}$$

$$\begin{aligned} &2\big[(u+c)(x-e)+v(y-f)\big]c\theta+ \\ &2\big[(u+c)(y-f)+v(e-x)\big]s\theta+ \\ &(u+c)^2+v^2+(x-e)^2+(y-f)^2-m^2=0, \end{aligned} \tag{10}$$

in which cosθ and sinθ are replaced with $c\theta$ and $s\theta$, respectively. The above two equations are quadratic with respect to x and y, therefore we consider an alternative equation that is linear with respect to x and y as well as cosθ and sinθ that can be obtained by subtracting Eq.(9) from Eq. (10) which gives:

$$\begin{aligned} &2\big[cx-fv-e(u+c)\big]c\theta+2\big[cy+ev-f(u+c)\big]s\theta+ \\ &+(u+c)^2+e^2-2xe-2yf-u^2+d^2+f^2-m^2=0. \end{aligned} \tag{11}$$

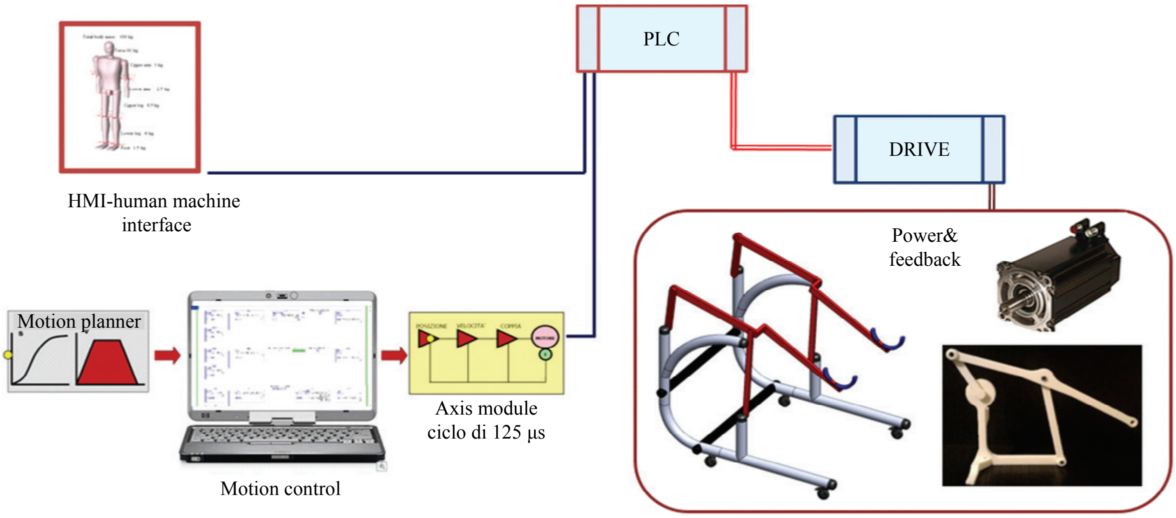

Fig. 9 A functional scheme of the overall mechatronic control system.

Table 2 Kinematic parameters of the mechanism in Fig. 5

Parameter	*d*	*m*	*c*	*u*	*v*	*e*	*f*
Dimension (mm]	668.0	310.3	606.4	675.2	54.2	579.0	527.4

The desired function can be obtained by eliminating θ, and further algebraic manipulations. In particular, the tan-half trigonometric identities are used, to get polynomial expressions of Eqs. (9) and (11) in a new variable t given in the form:

$$k_{11}t^2 - 2k_{12}t + k_{13} = 0,\ k_{11}t^2 - 2k_{12}t + k_{13} = 0, \tag{12}$$

where k_{ij} coefficients are function of design parameters only. t parameter can be eliminated from this system of two equations in Eq.(12) by dyalitic elimination method to get one single equation that is the coupler curve traced by point P that can be evaluated as the determinant of the matrix D in Eq. (13).

$$\boldsymbol{D} = \begin{bmatrix} k_{11} & -2k_{12} & k_{13} & 0 \\ k_{21} & -2k_{22} & k_{23} & 0 \\ 0 & k_{11} & -2k_{12} & k_{13} \\ 0 & k_{21} & -2k_{22} & k_{23} \end{bmatrix}. \tag{13}$$

The above-mentioned equation is function of the design parameters, x and y only. The design parameters of the synthesized mechanism obtained in the previous Section are reported in Table 2. Results of the formulation have been implemented to give the desired trajectory plotted together with the device of the sit-to-stand in Fig. 5 and the input link is m.

4.3 Functional mechatronic design

The described procedure can be used for a customization of the assisting device according to the anthropometric data of an individual. The designed mechanism has 1-DOF requiring a single actuator to give the desired trajectory. It is important to point out that in order to reproduce a natural movement also the speed of motion has to be controlled during the operation. A natural-like STS motion can be defined as a motion obtained by an individual without any external help. In particular, the execution speed can be modified by controlling the actuation, as described in the functional mechatronic control scheme reported in Fig. 9. In particular, the actuation motion law has to be prescribed in order to obtain suitable kinematic features in terms of velocity and acceleration of the point at the shoulder. In Fig. 9, the HMI interface can be used to set parameters referring to an individual and his/her physical conditions, together with any additional parameter of interest. In particular, the base frame and mechatronic components of the system are elements that do not change; and the support mechanism to generate the motion is designed ad-hoc. It is worth noting that according to the physical condition of the individual, the speed of the movement can be modified, while a change of the trajectory

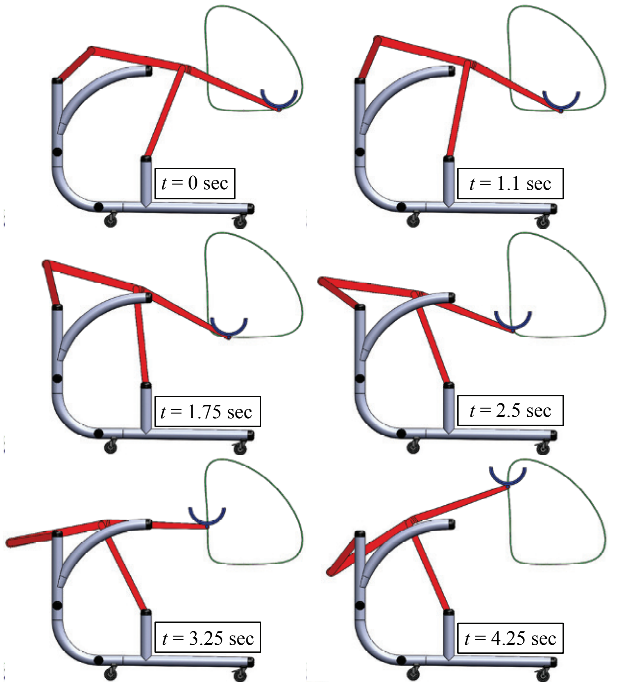

Fig. 10 A motion sequence for the proposed STS device.

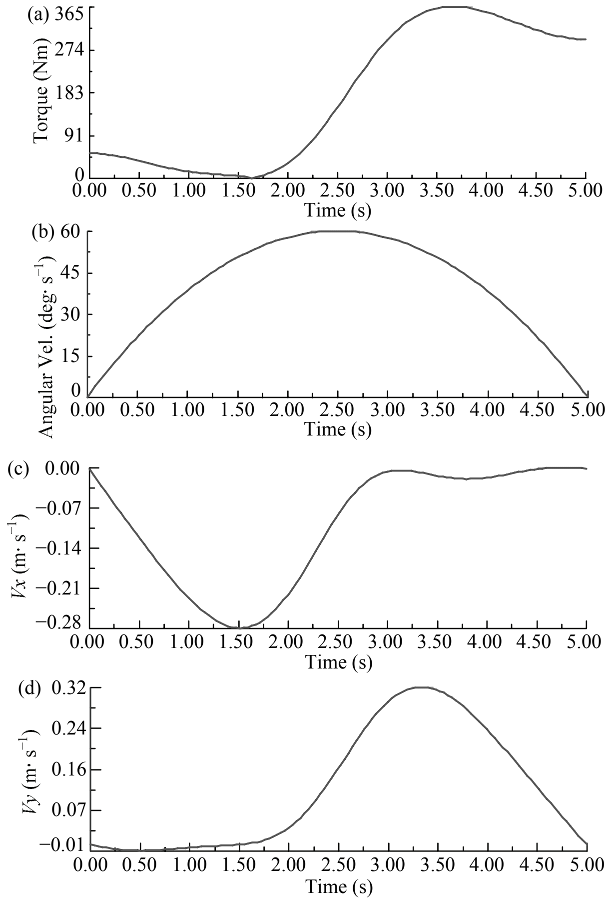

Fig. 11 Simulation numerical results. (a) Input torque; (b) angular velocity of the actuation; (c) x-components of an armpit point velocity; (d) y-component of an armpit point velocity.

requires a modification of the support mechanism. The information can be processed by a Motion Control block implemented on a PC. The PLC is connected with suitable drives to send signals and to operate the motors and receives the feedback from the sensors. Thus, it is possible to obtain a close-loop control in velocity, acceleration, or force[36,37]. Brushless motors may be selected because they have favorable characteristics for the application. Future development of this work will concern the realization of a prototype of the assisting device also implementing novel control strategies designed for systems with large payload variations, as in Refs. [38,39].

5 Numerical results

Fig. 10 shows a motion sequence for a simulation of the proposed design solution. The working range for the active joint of the support mechanism is 85˚, in particular it goes from 45˚, corresponding to t = 0 sec in Fig 10, to 230˚ when t = 4.25 s in Fig.10. It is worth noting that the sequence has been obtained without the model of the human body. Nevertheless, the influence of the body mass has been taken into account by adding forces acting on the device to perform the simulation and verification of the overturn of the system during the STS. More specifically, a verification of the stability of the system for overturn was carried out. The simulation was performed to test the system assuming an individual of 100 kg simulated with forces acting on the armpit support. Fig. 11 show the results of the simulation in terms of input torque, angular velocity, when a single motor is considered, and horizontal and vertical velocity components of a point attached to the armpit. The plots refer to the given range of 85˚, which is the working range of the mechanism during the STS. The simulation was carried out imposing a rotation of the active joint corresponding to the angular velocity in Fig. 11b. As expected, the maximum requested torque is in the lifting phase starting at t = 1.75 s.

6 Conclusion

In this paper, we proposed a functional design for customizing STS assisting devices, which may have a potential broad impact as much as the augment of the percentage of aged people in the world population. The STS action has been experimentally analyzed in order to identify suitable requirements for design purposes. Results of a trial considering adult volunteers, obtained with a motion capture system, were used for the design and simulation of a novel device. The transfer support mechanism has been selected as a four-bar linkage whose dimensions were calculated by a dimensional synthesis based on the Burmester problem. A procedure for customizing the design of STS devices has been detailed. Notice that, in the design procedure the base frame and mechatronic components of the system can be standardized; while the support mechanism to generate and sustain the body can be sized ad-hoc through dimensional synthesis to take into account anthropometric data of the subject understudy. Future development of this design is to build and test a prototype, involving participants with motor impairments or who use a walker.

References

[1] The Economist Intelligence Unit. The future of healthcare in Europe, [2017-11]. http://www.janssen- emea.com/ sites/ default/files/The%20Future%20Of%20Healthcare%20in%20Europe.pdf

[2] Chan A, Saito Y, Robine J M. International perspectives on summary measures of population health in an aging world. *Journal of Aging and Health*, 2016, **28**, 1119–1123.

[3] Mourex F, Pozzo T, Rouhier-Marcer I, Didier J-P. A kinematic comparison between elderly and young subjects standing up from and sitting down in a chair. *Journal of Age and Ageing*, 1998, **27**, 137–146.

[4] Nuzik S, Lamb R, Vansant A, Hirt S. Sit-to-stand movement pattern: A kinematic study. *Journal of Physical Therapy*, 1986, **66**, 1708–1713.

[5] Seedholm B B, Terayama K. Knee forces during the activity of getting out of a chair with and without the aid of the arms. *Journal of Biomedical Engineering*, 1976, **11**, 278–282.

[6] Burnfield J M, McCrory B, Shu Y, Buster T W, Taylor A P, Goldman A J. Comparative kinematic and electromyographic assessment of clinician- and device-assisted sit-to-stand transfers in patients with stroke. *Physical Therapy*, 2013, **93**, 1331–1341.

[7] Palopoli L, Argyros A, Birchbauer J, Colombo A, Fontanelli D, Legay A, Garulli A, Giannitrapani A, Macii D, Moro F, Nazemzadeh P, Padeleris P, Passerone R, Poier G, Prattichizzo D, Rizano T, Rizzon L, Scheggi S, Sedwards S. Navigation assistance and guidance of older adults across complex public spaces: The DALi approach. *Intelligent Service Robotics*, 2015, **8**, 77–92.

[8] Nagai K, Nakanishi I, Hanafusa H. Assistance of self-transfer of patients using a power-assisting device. *IEEE International Conference on Robotics* & *Automation*, Taipei, Taiwan, 2003, 4008–4015.

[9] Hirata Y, Higuchi J, Hatsukari T, Kosuge K. Sit-to-stand assist system by using handrail and electric bed moving up and down. 2*nd IEEE RAS EMBS International Conference on Biomedical Robotics and Biomechatronics*, Scottsdale, AZ, USA, 2008, 187–192.

[10] Jun H G, Chang Y Y, Dan B J, Jo B R, Min B H, Yang H, Song W K, Kim J. Walking and sit-to-stand support system for elderly and disabled. *IEEE International Conference on Rehabilitation Robotics* (*ICORR*), Zurich, Switzerland, 2011, 1–5.

[11] DallaLibera F, Tsusaka Y, Okazaki Y, Futakuchi R, Yamamoto M, Shikata N, Terashima M. Analysis of velocity's influence on forces and muscular activity in the context of sit-to-stand motion assisted by an elderly care robot. *IEEE International Conference on Intelligent Robots and Systems*, Daejeon, Korea, 2016, 717–724.

[12] Schiffer S, Ferrein A Lakemeyer G. Caesar: An intelligent domestic service robot. *Intelligent Service Robotics*, 2012, **5**, 259–273.

[13] Martins M M, Santos C P, Frizera-Neto, A, Ceres R. Assistive mobility devices focusing on smart walkers: Classification and review. *Robotics and Autonomous Systems*, 2012, **60**, 548–562.

[14] Krishnan R H, Pugazhenthi S. Mobility assistive devices and self-transfer robotic systems for elderly, a review. *Intelligent Service Robotics*, 2014, **7**, 37–49.

[15] Onishi M, Luo Z, Odashima T, Hirano S, Tahara K, Mukai T. Generation of human care behaviors by human-interactive robot RI-MAN. *Proceedings* 2007 *IEEE International Conference on Robotics and Automation*, Rome, Italy, 2007, 3128–3129.

[16] Tsukahara A, Kawanishi R, Hasegawa Y, Sankai Y. Sit-to-stand and stand-to-sit transfer support for complete paraplegic patients with robot suit hal. *Advanced Robotics*, 2010, **24**, 1615–1638.

[17] Topro Taurus Walker, [2017-11], http://www.mobilitycare.net.au/buy/topro-taurus/

[18] Purwar A, Galeotafiore T, Miles J, Renert J. *Portable Six-bar Apparatus for Llifting*, *Lowering and Self-propelled*

Iransit, US patent, No. 8468622B2, 2011.

[19] Wang Q, Kurillo G, Ofli F, Bajcsy R. Evaluation of pose tracking accuracy in the first and second generations of microsoft kinect. *IEEE International Conference on Healthcare Informatics* 2015 (*ICHI* 2015), Dallas, TX, USA, 2015, 380–389

[20] Rea P, Ottaviano E, Conte M, D'Aguanno A, De Carolis D. The design of a novel tilt seat for inversion therapy. *International Journal of Imaging and Robotics*, 2013, **11**, 1–10,

[21] Rea P, Ottaviano E, Castelli G. A procedure for the design of novel assisting devices for the Sit-to-Stand. *Journal of Bionic Engineering*, 2013, **10**, 488–496.

[22] Timmi A, Pennestrì E, Valentini P P, Aschieri P. Biomechanical analysis of two variants of the Karate reverse punch (Gyaku Tsuki) based on the evaluation of the body kinetic energy from 3D mocap data. *Proceedings of Multibody Dynamics*, *ECCOMAS*, Brussels, Belgium, 2011.

[23] Virtual Sensei, [2017-11], http://www.virtualsensei.it/.

[24] Vaida C, Plitea N, Cocorean D, Pisla D. Modeling of new spatial parallel structures with constant platform orientation using planar parallel modules. *Proeedings of the Romanian Academy*, *Series A*, 2014; **15**, 43–51.

[25] Ottaviano E Ceccarelli M, Castelli G. Experimental results of a 3-DOF parallel manipulator as an earthquake motion simulator. *ASME Design Engineering Technical Conferences and Computers and Information in Engineering Conference*, Salt Lake City, USA, 2004.

[26] Thomas F, Ottaviano E, Ros L, Ceccarelli M. Performance analysis of a 3-2-1 pose estimation device. *IEEE Transactions on Robotics*, 2005, **21**, 288–297.

[27] McCarthy J M, Joskowicz L. *Kinematic Synthesis*, Cambridge University Press, New York, USA, 2001.

[28] Hall A S. *Kinematics and Linkage Design*, Waveland Press. Inc., Prospect Heights, Illinois, USA, 1961.

[29] Hunt K H. *Kinematic Geometry of Mechanisms*, Oxford University Press, New York, USA, 1990.

[30] Shoup T E. Centrodes of the slider-crank mechanism. 8*th IFToMM World Conference on the Theory of Machines and Mechanisms*, Prague, Czech Republic, 1991, **1**, 59–62.

[31] Bottema O, Roth B. *Theoretical Kinematics*, North-Holland Publishing Company, New York, USA, 1979.

[32] McCarthy J M. *Geometric Design of Linkages*, Springer-Verlag, New York, USA, 2000.

[33] Sandor G N, Erdman A. *Advanced Mechanism Design*: *Analysis and Synthesis Vol*. II, Prentice-Hall, Inc., New Jersey, USA, 1984.

[34] Ravani B, Roth B. Motion synthesis using kinematic mappings. *ASME Journal of Mechanism*, *Transmissions*, *and Automation in Design*, 1983, **105**, 460–467.

[35] Al-Widyan K, Angeles J, Cervantes-Sánchez J J. A numerically robust algorithm to solve the five-pose Burmester problem. *ASME* 2002 *International Design Engineering Technical Conferences and Computers and Information in Engineering Conference*, Montreal, Quebec, Canada, 2002, 617–626.

[36] Figliolini G, Rea P. Ca.U.M.Ha. robotic hand (Cassino-Underactuated-Multifinger-Hand). 2007 *IEEE*/*ASME International Conference on Advanced Intelligent Mechatronics* (*AIM*2007), Zurich, Switzerland, 2007.

[37] Figliolini G, Rea P. Overall design of Ca.U.M.Ha. robotic hand for harvesting horticulture products. *Robotica*, 2006, **24**, 329–331.

[38] Feliu V, Castillo F J, Jaramillo V, Partida G. A robust controller for a 3-DOF flexible robot with a time variant payload. *Asian Journal of Control*, 2013, **15**, 971–987.

[39] Feliu V, Castillo F J, Ramos F, Somolinos J A. Robust tip trajectory tracking of a very lightweight single-link flexible arm in presence of large payload changes. *Mechatronics,* 2012, **22**, 594–613.